Evolution of early male-killing in horizontally transmitted parasites

Supplementary Material

Veronika Bernhauerová[1,*], Luděk Berec[2,3], and Daniel Maxin[4]

[1]Department of Mathematics and Statistics, Faculty of Science, Masaryk University, Kotlářská 2, 61137 Brno, Czech Republic, E-mail: bernhauerv@gmail.com

[2]Department of Biosystematics and Ecology, Institute of Entomology, Biology Centre CAS, Branišovská 31, 37005 České Budějovice, Czech Republic, E-mail: berec@entu.cas.cz

[3]Institute of Mathematics and Biomathematics, Faculty of Science, University of South Bohemia, Branišovská 1760, 37005 České Budějovice, Czech Republic

[4]Department of Mathematics and Statistics, Valparaiso University, 1900 Chapel Drive, Valparaiso, IN 46383, USA, E-mail: daniel.maxin@valpo.edu

[*]To whom correspondence should be addressed.

Appendix S1 Stability of host extinction and disease-free equilibra of the model (1)

Incorporating the mating function $\mathcal{M}(F,M) = 2c\frac{FM}{F/h+M}$ into the model (1) in the main text, we have

$$\begin{aligned}
\frac{dF_u}{dt} &= c\frac{[F_u+(1-\xi)rF_i](M_u+M_i)}{(F_u+F_i)/h+M_u+M_i} - \lambda F_u(F_i+M_i) - (\mu+bP)F_u \\
\frac{dM_u}{dt} &= c\frac{[F_u+(1-\xi)rF_i](M_u+M_i)}{(F_u+F_i)/h+M_u+M_i} - \lambda M_u(F_i+M_i) - (\mu+bP)M_u \\
\frac{dF_i}{dt} &= cr\xi\frac{F_i(M_u+M_i)}{(F_u+F_i)/h+M_u+M_i} + \lambda F_u(F_i+M_i) - (\mu+bP)F_i - \alpha F_i \\
\frac{dM_i}{dt} &= cr\xi(1-q)\frac{F_i(M_u+M_i)}{(F_u+F_i)/h+M_u+M_i} + \lambda M_u(F_i+M_i) - (\mu+bP)M_i - \alpha M_i
\end{aligned} \tag{S1.1}$$

See also Table S 2 for details on the male-killing process. Notice that if $F_u(0) = M_u(0)$, then $F_u(t) = M_u(t)$ for all $t > 0$. Therefore, we can reduce the number of equations in the model (S1.1) from four to three, introducing a variable S as the total density of the uninfected individuals and noting that

$$F_u = M_u = \frac{S}{2}$$

The reduced model then is

$$\begin{aligned}
\frac{dS}{dt} &= \frac{2c}{(\frac{S}{2}+F_i)/h+\frac{S}{2}+M_i}\left[\left(\frac{S}{2}+M_i\right)\left(\frac{S}{2}+(1-\xi)rF_i\right)\right] - \lambda S(F_i+M_i) - (\mu+bP)S \\
\frac{dF_i}{dt} &= cr\xi\frac{F_i\left(\frac{S}{2}+M_i\right)}{(\frac{S}{2}+F_i)/h+\frac{S}{2}+M_i} + \lambda\frac{S}{2}(F_i+M_i) - (\mu+bP)F_i - \alpha F_i \\
\frac{dM_i}{dt} &= cr\xi(1-q)\frac{F_i\left(\frac{S}{2}+M_i\right)}{(\frac{S}{2}+F_i)/h+\frac{S}{2}+M_i} + \lambda\frac{S}{2}(F_i+M_i) - (\mu+bP)M_i - \alpha M_i
\end{aligned} \tag{S1.2}$$

Now we briefly present a stability analysis of the host extinction and disease-free equilibria corresponding to the model (S1.2).

Appendix S1.1 Host extinction equilibria and their stability

Since the model (S1.2) is not differentiable at the origin we construct an equivalent system in terms of the proportion of infected females $x = \frac{F_i}{P}$, the proportion of infected males $y = \frac{M_i}{P}$, and the total host density P which will permit linearisation around $P = 0$. The equivalent model is as follows:

$$\frac{dx}{dt} = \frac{chx(1-x+y)}{1+h+(1-h)(x-y)}[r\xi - 1 + x + y - (2r - r\xi q)x] + \frac{\lambda}{2}P(1-x-y)(x+y) - \alpha x(1-x-y)$$

$$\frac{dy}{dt} = \frac{ch(1-x+y)}{1+h+(1-h)(x-y)}\{r\xi(1-q)x - y[1-x-y+(2r-r\xi q)x]\} + \frac{\lambda}{2}P(1-x-y)(x+y) - \alpha y(1-x-y)$$

$$\frac{dP}{dt} = \left\{\frac{ch(1-x+y)}{1+h+(1-h)(x-y)}[1-x-y+(2r-r\xi q)x] - \alpha(x+y) - \mu - bP\right\}P \tag{S1.3}$$

This model has five host extinction equilibria: $(0,0,0)$, $(1,0,0)$, $(0,1,0)$, $\left(0, \frac{ch+(1+h)\alpha}{\alpha-(c+\alpha)h}, 0\right)$, and $(x^*, y^*, 0)$ (see Figs. S 1 and S 2 for illustration) with $y^* = (1-q)x^*$ and x^* as a root of

$$Ax^2 + Bx + C = 0$$

where

$$A = [h(c+\alpha) - \alpha - chr\xi]q^2 + 2q[chr + \alpha - h(c+\alpha)]$$

$$B = 2ch(1-r) + 2\alpha(1+h) - 2\alpha q$$

$$C = ch(r\xi - 1) - \alpha(1+h)$$

Denoting $J(x,y,P)$ the Jacobian matrix of the model (S1.3) we now summarize stability properties of these host extinction equilibria in a series of propositions. We assume $ch/(1+h) > \mu$ to avoid host extinction in the absence of any infection.

Proposition 1. *The extinction equilibrium* $(0,0,0)$ *is always unstable.*

Proof. The Jacobian matrix $J(0,0,0)$ of the model (S1.3) is diagonal with the eigenvalues

$$\frac{ch(r\xi-1)}{1+h},\ -\frac{ch}{1+h} - \alpha,\ \frac{ch}{1+h} - \mu$$

Since the last eigenvalue is positive for $ch/(1+h) > \mu$, the extinction equilibrium $(0,0,0)$ is always unstable. □

Proposition 2. *The extinction equilibrium* $(1,0,0)$ *is always unstable.*

Proof. The Jacobian matrix $J(1,0,0)$ of the model (S1.3) is a block matrix with one negative eigenvalue $-\alpha-\mu$ and two other eigenvalues whose sum is $\alpha+chr(1-q\xi)>0$. This means that the latter two eigenvalues are either complex conjugate with positive real part or real with at least one of them positive. The extinction equilibrium $(1,0,0)$ is thus always unstable. □

Proposition 3. *The extinction equilibrium* $(0,1,0)$ *is always unstable.*

Proof. The Jacobian matrix $J(0,1,0)$ of the model (S1.3) is upper diagonal and its eigenvalues are $cr\xi$, $c+\alpha$ and $-\alpha-\mu$. Since the first two eigenvalues are positive, the extinction equilibrium $(0,1,0)$ is always unstable. □

Proposition 4. *The extinction equilibrium* $\left(0, \frac{ch+(1+h)\alpha}{\alpha-(c+\alpha)h}, 0\right)$ *is never feasible.*

Proof. The statement directly follows from the observation that the inequality

$$0 < \frac{ch+(1+h)\alpha}{\alpha-(c+\alpha)h} < 1$$

ensuring feasibility of the equilibrium holds if and only if $c<-\alpha$. However, this latter inequality can never be satisfied as all model parameters are assumed positive. □

Proposition 5. *Let* $\xi=h=1$. *Then there is a stable extinction equilibrium* $(x^*,y^*,0)$.

Proof. With $h=\xi=1$ we have two possible roots for x^*:

$$x_1^*=\frac{1}{2-q} \quad \text{and} \quad x_2^*=\frac{c(r-1)-2\alpha}{cq(r-1)}$$

Moreover, $y_1^*=(1-q)x_1^*$ and $y_2^*=(1-q)x_2^*$.

The equilibrium $(x_1^*,y_1^*,0)$ is always feasible and the Jacobian matrix $J(x_1^*,y_1^*,0)$ of the model (S1.3) has the following eigenvalues

$$-\frac{cr(1-q)}{2-q},\ \frac{cr(q-1)+\alpha(2-q)+\mu(2-q)}{q-2},\ \frac{c(r-1)(1-q)-\alpha(2-q)}{q-2}$$

While the first eigenvalue is always negative, the latter two eigenvalues are negative provided that

$$\mu > cr\frac{1-q}{2-q}-\alpha \quad \text{and} \quad c>\frac{\alpha(2-q)}{(r-1)(1-q)}$$

This means that the death rate μ is large enough to cause extinction and the birth rate c is large enough to maintain positive proportions of infected females and males.

Turning to the equilibrium $(x_2^*, y_2^*, 0)$ we notice that the feasibility condition $0 < x_2^* < 1$ implies

$$2\alpha < c(r-1) < \frac{2\alpha}{1-q} \tag{S1.4}$$

Then the eigenvalues of the Jacobian matrix $J(x_2^*, y_2^*, 0)$ are

$$-\frac{r\alpha}{r-1},\ \frac{\alpha}{r-1} - \mu,\ \frac{[c(r-1)-2\alpha][c(r-1)(1-q)-\alpha(2-q)]}{cq(r-1)}$$

The first eigenvalue is always negative. Imposing that the latter two eigenvalues are negative and taking into account the feasibility condition (S1.4), we arrive to the following stability condition

$$\mu > \frac{\alpha}{r-1} \quad \text{and} \quad \frac{2\alpha}{r-1} < c < \frac{\alpha(2-q)}{(r-1)(1-q)}$$

□

Appendix S1.2 Disease-free equilibrium and its stability

Going back to the original model (S1.2) defined in terms of the variables S, F_i and M_i, there is a unique disease-free equilibrium (DFE)

$$F_i^* = 0,\ M_i^* = 0,\ S^* = \frac{1}{b}\left(\frac{ch}{1+h} - \mu\right)$$

Notice that whenever the DFE is feasible ($S^* > 0$) then the extinction equilibrium $(0, 0, 0)$ of the equivalent model (S1.3) is unstable.

The Jacobian matrix of the model (S1.2) evaluated at the DFE has three eigenvalues. One is $-\left(\frac{ch}{1+h} - \mu\right)$ which is always negative. The other two, denoted by e_1 and e_2, have the following sum and product

$$e_1 + e_2 = \frac{1}{b(1+h)}\{\lambda[ch - \mu(h+1)] + bch(r\xi - 2) - 2\alpha b(1+h)\}$$

$$e_1 e_2 = \frac{1}{b(1+h)^2}(\lambda M + N)$$

where

$$M = \frac{1}{2}[ch - \mu(h+1)][(cr\xi q - 2c - 2\alpha)h - 2\alpha]$$

$$N = -b[(cr\xi - c - \alpha)h - \alpha][ch + \alpha(1+h)]$$

The condition $e_1 + e_2 < 0$ implies

$$\frac{\lambda}{b} < \frac{2\alpha(1+h) + ch(2-r\xi)}{ch - \mu(h+1)} \tag{S1.5}$$

This condition requires its right side to be positive which is always true for $\xi < 1$, since $r \leq 2$. This allows us to rewrite the condition $e_1 e_2 > 0$ as

$$\frac{\lambda}{b} < \frac{2[(c - cr\xi + \alpha)h + \alpha][ch + \alpha(1+h)]}{[ch - \mu(h+1)][ch(2 - r\xi q) + 2\alpha(1+h)]} \tag{S1.6}$$

One can show that the right side of (S1.6) is smaller than the right side of (S1.5). Therefore, combining these two inequalities, we obtain the following necessary and sufficient condition for stability of the DFE:

$$\frac{\lambda}{b} < \frac{2[(c - cr\xi + \alpha)h + \alpha][ch + \alpha(1+h)]}{[ch - \mu(h+1)][ch(2 - r\xi q) + 2\alpha(1+h)]}$$

Appendix S1.3 The special case $\xi = q = 1$ and $\lambda = \alpha = 0$

For the special case of $\xi = q = 1$ and $\lambda = \alpha = 0$, which corresponds to a fully efficient MK bacterium transmitted purely vertically with 100% efficacy, the model (S1.2) simplifies to (note that $r = 1 + \gamma$ in this case):

$$\begin{aligned}
\frac{dS}{dt} &= \frac{2c}{(F_u + F_i)/h + M_u + M_i}\left(\frac{S}{2} + M_i\right)\frac{S}{2} - (\mu + bP)S \\
\frac{dF_i}{dt} &= \frac{c(1+\gamma)}{(F_u + F_i)/h + M_u + M_i}F_i\left(\frac{S}{2} + M_i\right) - (\mu + bP)F_i \\
\frac{dM_i}{dt} &= -(\mu + bP)M_i
\end{aligned} \tag{S1.7}$$

We show that in this case the host population always goes extinct. First notice that $\frac{dM_i}{dt} < -\mu M_i$ which implies that M_i approaches zero density. Assuming that the infected male population has gone extinct the dynamics is given by the following planar system:

$$\begin{aligned}
\frac{dS}{dt} &= \frac{c}{(S/2 + F_i)/h + S/2}\frac{S^2}{2} - (\mu + bP)S \\
\frac{dF_i}{dt} &= \frac{c(1+\gamma)}{(S/2 + F_i)/h + S/2}F_i\frac{S}{2} - (\mu + bP)F_i
\end{aligned} \tag{S1.8}$$

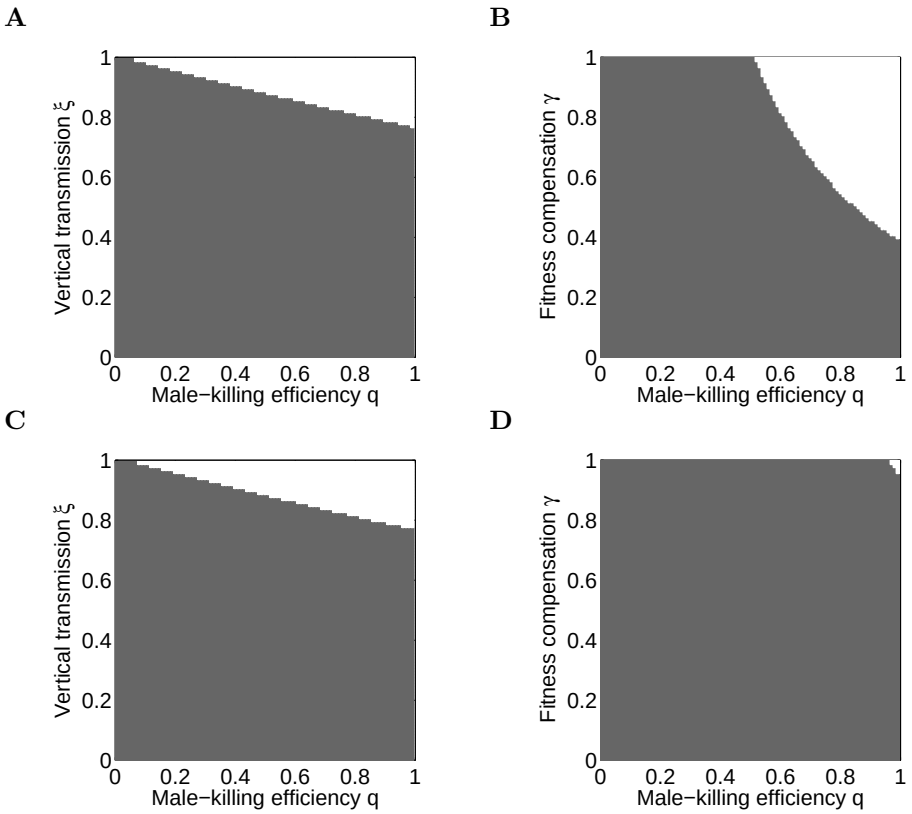

Figure S 1: Existence and stability of host extinction equilibria for $\lambda = 0.1$. Grey colour = no extinction equilibrium, white colour = one unstable extinction equilibrium. Parameters: (A) $h = 1$, $\gamma = 0.5$, (B) $\xi = 0.8$, $h = 1$, (C) $h = 0.52$, $\gamma = 0.5$, (D) $\xi = 0.68$, $h = 0.52$. Common parameters: $a_2 = 0.5$, all other parameters are given in Table S 1.

This is equivalent to the following system defined in terms of the variables $x = \frac{S}{S+F_i}$ and $P = S + F_i$:

$$\begin{aligned} \frac{dx}{dt} &= ch\gamma \frac{x(1-x)^2}{1+h+x(1-h)} \\ \frac{dP}{dt} &= \left[ch\frac{(1-x)(1+\gamma x)}{1+h+x(1-h)} - (\mu + bP) \right] P \end{aligned} \tag{S1.9}$$

Since the first equation is independent of P we can analyse it separately. It is easy to see that $\dfrac{dx}{dt} \geq 0$ in the feasible invariant domain $0 \leq x \leq 1$ and that the only equilibria for x are 0 and 1. Since x is an increasing function of time it follows that $x(t)$ has to approach 1. Using this limit, we have that

$$\lim_{t\to\infty} \frac{1}{P}\frac{dP}{dt} < -\mu < 0$$

which shows that $P(t)$ approaches zero density, that is, that the host population goes extinct.

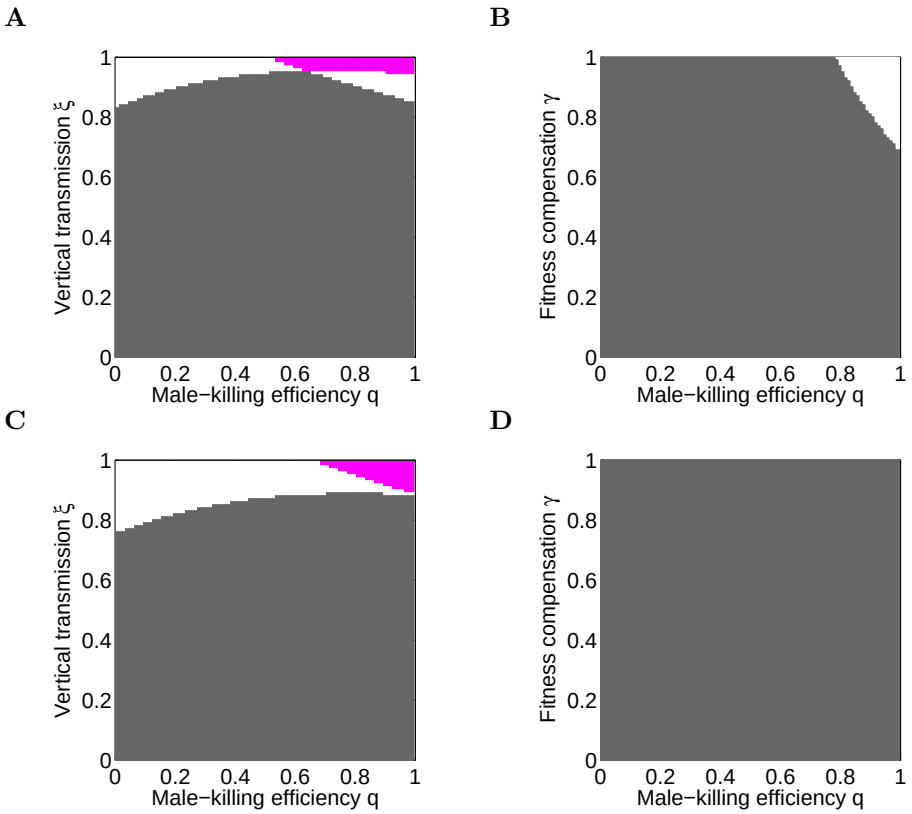

Figure S 2: Existence and stability of host extinction equilibria for $\lambda = 0.5$. Grey colour = no extinction equilibrium, white colour = one unstable extinction equilibrium, magenta colour = two extinction equilibria, both unstable. Parameters: (A) $h = 1$, $\gamma = 0.5$, (B) $\xi = 0.8$, $h = 1$, (C) $h = 0.52$, $\gamma = 0.5$, (D) $\xi = 0.68$, $h = 0.52$. Common parameters: $a_2 = 0.5$, all other parameters are given in Table S 1.

Appendix S2 Essential components of the model (1)

The model (1) in the main text contains several essential components which we at large discuss here.

Appendix S2.1 Benefit from male-killing

Early male-killing (MK) incurs a cost on the infected hosts in the form of reduced fecundity of infected females, but at the same time confers a benefit to the surviving host offspring in terms of decreased competition between them. The benefit comes either from the freed resources that would otherwise go to the dead males and are now redistributed to the surviving offspring, or through consumption of the dead male eggs [1–3]. As a result, more females capable of spreading the male-killer survive in the clutch. Given the vertical transmission (VT) efficacy ξ, positive relationship between the fitness benefit r allocated to the surviving

offspring and the MK efficacy q can be expressed as [1, 4]

$$r = 1 + \gamma \frac{q\xi/2}{1 - q\xi/2} \tag{S2.1}$$

where $0 \leq \gamma \leq 1$ is the fraction of freed resources that can be redistributed among the surviving offspring (further referred to as the "fitness compensation parameter"). Note that the freed resources are not available just to the infected female offspring, but also to the surviving infected male offspring as well as to the uninfected progeny. Also, the benefit conferred by MK adds only through fecundity.

Appendix S2.2 Trade-offs

To investigate the evolution of MK in an originally virulent non-MK parasite that is transmitted both vertically and horizontally, we assume that the parasite-induced host mortality α (further referred to as virulence), the horizontal transmission (HT) rate λ and the VT efficacy ξ are all affected by the parasite's "exploitation strategy" of the host, a pleiotropic trait $\epsilon > 0$. The variable ϵ is a dummy variable rather than a trait with any direct biological interpretation [5, 6]. For simplicity, we let the virulence to be proportional to the exploitation strategy,

$$\alpha(\epsilon) = a_\alpha \epsilon, \quad a_\alpha > 0 \tag{S2.2}$$

reflecting that increased exploitation of the host by the parasite is accompanied by an increased harm to the host. The rate of HT is assumed to increase with the parasite's exploitation strategy as

$$\lambda(\epsilon) = \lambda_{\min} + (\lambda_{\max} - \lambda_{\min})\epsilon^{a_2} \tag{S2.3}$$

The parameters $0 \leq \lambda_{\min} < \lambda_{\max}$ are, respectively, the minimum and maximum rates of HT set by any phylogenetic constraint and $a_2 > 0$ is a constant controlling the shape of (S2.3). Finally, we assume the VT efficacy to decrease with increasing exploitation strategy as

$$\xi(\epsilon) = \xi_{\min} + (\xi_{\max} - \xi_{\min})(1 - (\epsilon^{a_2})^z)^{1/z} \tag{S2.4}$$

Here, $0 \leq \xi_{\min} < \xi_{\max} \leq 1$ are, respectively, the minimum and maximum VT efficacies. The parameter $z > 0$ can be viewed to express a cost of VT in the sense of how much the HT rate can increase when small if the VT efficacy drops by a value. With this interpretation, we will refer to an increase in the parameter z as to a decrease in the cost of VT ($z < 1$, cheap VT), and a decrease in z as an increase in the cost of VT ($z > 1$, costly VT).

To avoid following the dummy variable ϵ, we combine (S2.2) and (S2.3) together to obtain

a trade-off between the parasite virulence α and HT rate λ as

$$\alpha(\lambda) = \left(\frac{\lambda - \lambda_{\min}}{a_1} \right)^{1/a_2} \tag{S2.5}$$

where $a_1 = (\lambda_{\max} - \lambda_{\min})/a_\alpha^{a_2}$. Note that α is a convex (or concave) function of λ for $0 < a_2 < 1$ (or $a_2 > 1$). Similarly, by combining (S2.3) and (S2.4) we obtain a trade-off between the VT efficacy ξ and HT rate λ as

$$\xi(\lambda) = \xi_{\min} + (\xi_{\max} - \xi_{\min}) \left(1 - \left(\frac{\lambda - \lambda_{\min}}{\lambda_{\max} - \lambda_{\min}} \right)^z \right)^{1/z} \tag{S2.6}$$

Similarly, ξ is a convex (or concave) function of λ for $z < 1$ (or $z > 1$). A trade-off between vertical and horizontal modes of transmission has long been hypothesized [7, 8], modelled [9–11], and later also found to exist in plant parasites [12, 13] and plasmids [14, 15].

Appendix S2.3 Mating function

The mating system of a species is largely shaped by the number of males and females willing to mate at any given time [16]. In this regard, it has been hypothesized that sex ratio distorters, such as MK bacteria, may induce reproductive evolution of their hosts, including sex-role reversal [17–19]. Charlat et al. [19] also reported that an increasing female bias in the host population caused by a MK *Wolbachia* strain might lead to an increase in female mating frequency until the diminishing male sperm resources would become limiting at extreme female biases.

Here, we explore the opposite direction: we assume a mating system to be established and let the male-killer adapt to it. Since we do not consider an agent-based model explicitly accounting for harems or mating dominance in individual males and females, we address this issue phenomenologically. To account for a wide range of mating systems, we consider a frequently used and empirically supported harmonic mean function as a description of pair bonding rate [20–23]. This function depends on the densities of females (F) and males (M),

$$\mathcal{M}(F, M) = 2c \, \frac{FM}{F/h + M} \tag{S2.7}$$

where c is the per-mating number of offspring (birth rate). The mating system is controlled by the parameter h; $h < 1$ corresponds to polyandry, $h = 1$ corresponds to monogamy, and $h > 1$ corresponds to polygyny [20]. Indeed, with polygyny, each male can mate with up to h females, so there are effectively h times more males available for females than in the case of monogamy and the mating rate is $cF(hM)/((F + hM)/2) = cFM/((F/h + M)/2)$.

With polyandry, each female can mate with up to k males, so there are effectively k times less males available for females than in the case of monogamy. The mating rate is then $cF(M/k)/((F + M/k)/2) = cFM/((kF + M)/2)$. If we set $h = 1/k$, we get a common mating rate $cFM/((F/h + M)/2)$.

Appendix S3 Male-killing in purely vertically transmitted bacteria

Here, we consider a bacterium that is transmitted purely vertically. A strain with the male-killing efficacy q can invade the completely susceptible host population if its basic reproduction number is greater than one,

$$R_0(q) = \xi r(q) > 1 \tag{S3.1}$$

and dies out otherwise. Therefore, persistence of the male-killer depends only on the vertical transmission efficacy ξ, fitness compensation parameter γ, and male-killing efficacy q. In addition, the persistence condition (S3.1) says that if the bacterium is not beneficial to its host ($\gamma = 0$) then male-killers cannot invade the host regardless of the vertical transmission efficacy ξ and male-killing efficacy q.

The invasion analysis [24] yields the fitness proxy of a mutant $\hat{q}$ in the environment formed by a resident q as

$$f(\hat{q}, q) = \frac{r(\hat{q})}{r(q)} - 1 \tag{S3.2}$$

The mutant strain $\hat{q}$ can invade the resident strain q if $r(\hat{q}) > r(q)$ which is satisfied once $\hat{q} > q$. Therefore, strains with higher male-killing efficacy will keep invading and outcompeting less efficient strains until they reach the full male-killing efficacy $q = 1$ (Fig. S 3A). Note, that if a bacterium is to become a resident, it has to be viable, that is, it has to have $R_0(q) > 1$ which is fulfilled once $\xi r(q) > 1$ (see the condition (S3.1)). However, the bacterium is not viable for all values of q if $\xi < 1$ (Fig. S 3A). This implies that highly efficient male-killers cannot evolve from less efficient and thus non-viable strains. The full male-killing efficacy $q = 1$ can be reached by gradual evolution only if the bacterium is transmitted vertically with 100% efficacy ($\xi = 1$), which is unlikely to be the case of current male-killing bacteria observed in nature. In particular, this would impose extinction of the host (see section Appendix S1.3 in Appendix S1 for details).

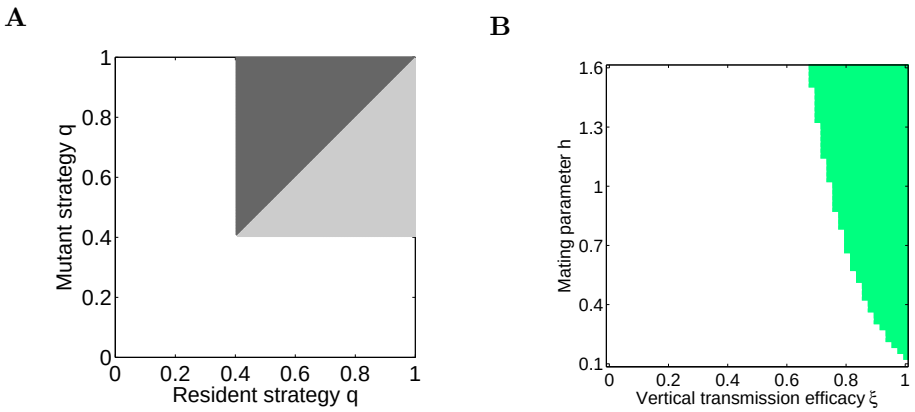

Figure S 3: When there is no horizontal transmission of the bacterium ($\lambda = 0$), and thus no virulence ($\alpha = 0$), then the only evolutionary endpoint is $q = 1$. (A) Pairwise invasibility plot. Dark grey colour = positive invasion fitness, light grey colour = negative invasion fitness, white colour = non-persistence of the male-killer. Parameters: $\xi = 0.8$, $\gamma = 0.5$. (B) Region of the parameter space in which the bacterium is viable for at least some values of q (green). All other parameters are given in Table S 1.

Appendix S4 Evolution of horizontal transmission rate λ

We now calculate the invasion fitness proxy $f(\hat{\lambda}, \lambda)$ of a rare mutant possessing the strategy $\hat{\lambda}$ in the environment formed by a resident λ provided that the bacterium has not yet evolved any male-killing property (thus $q = 0$). The resident-mutant dynamics are given as

$$\begin{aligned}
\frac{dS}{dt} &= \frac{2c}{(\frac{S}{2}+F_i+\hat{F}_i)/h+\frac{S}{2}+M_i+\hat{M}_i}\left[\left(\frac{S}{2}+M_i+\hat{M}_i\right)\left(\frac{S}{2}+(1-\xi)(F_i+\hat{F}_i)\right)\right] \\
&\quad -\lambda(F_i+M_i)S-\hat{\lambda}(\hat{F}_i+\hat{M}_i)S-(\mu+bP)S \\
\frac{dF_i}{dt} &= c\xi\frac{F_i\left(\frac{S}{2}+M_i+\hat{M}_i\right)}{(\frac{S}{2}+F_i+\hat{F}_i)/h+\frac{S}{2}+M_i+\hat{M}_i}+\lambda(F_i+M_i)\frac{S}{2}-(\mu+bP)F_i-\alpha F_i \\
\frac{dM_i}{dt} &= c\xi\frac{F_i\left(\frac{S}{2}+M_i+\hat{M}_i\right)}{(\frac{S}{2}+F_i+\hat{F}_i)/h+\frac{S}{2}+M_i+\hat{M}_i}+\lambda(F_i+M_i)\frac{S}{2}-(\mu+bP)M_i-\alpha M_i \\
\frac{d\hat{F}_i}{dt} &= c\xi\frac{\hat{F}_i\left(\frac{S}{2}+M_i+\hat{M}_i\right)}{(\frac{S}{2}+F_i+\hat{F}_i)/h+\frac{S}{2}+M_i+\hat{M}_i}+\hat{\lambda}(\hat{F}_i+\hat{M}_i)\frac{S}{2}-(\mu+bP)\hat{F}_i-\hat{\alpha}\hat{F}_i \\
\frac{d\hat{M}_i}{dt} &= c\xi\frac{\hat{F}_i\left(\frac{S}{2}+M_i+\hat{M}_i\right)}{(\frac{S}{2}+F_i+\hat{F}_i)/h+\frac{S}{2}+M_i+\hat{M}_i}+\hat{\lambda}(\hat{F}_i+\hat{M}_i)\frac{S}{2}-(\mu+bP)\hat{M}_i-\hat{\alpha}\hat{M}_i
\end{aligned} \tag{S4.1}$$

Here $\hat{F}_i$ and $\hat{M}_i$ denote densities of female and male hosts affected by a mutant male-killer, respectively. The Jacobian matrix of the submodel corresponding to the last two equations of the model (S4.1) is

$$J_{mut} = \begin{pmatrix} c\xi P_T^* + \hat{\lambda}\frac{S^*}{2} - (\mu + bP^*) - \hat{\alpha} & \hat{\lambda}\frac{S^*}{2} \\ c\xi P_T^* + \hat{\lambda}\frac{S^*}{2} & \hat{\lambda}\frac{S^*}{2} - (\mu + bP^*) - \hat{\alpha} \end{pmatrix} \tag{S4.2}$$

with $P_T^* = (\frac{S^*}{2} + M_i^*)/[(\frac{S^*}{2} + F_i^*)/h + \frac{S^*}{2} + M_i^*]$ where $P^* = S^* + F_i^* + M_i^*$.

Using the Next-Generation-Theorem (NGT) to calculate the largest eigenvalue of J_{mut} we decompose the matrix (S4.2) such that $J_{mut} = F - V$ where F is the matrix of all terms representing creation of new infected individuals (birth rates and transitions from the uninfected class to the infected class) and V is the matrix of all terms representing removal of individuals (death rates) [24]. Therefore, we have

$$F = \begin{pmatrix} c\xi P_T^* + \hat{\lambda}\frac{S^*}{2} & \hat{\lambda}\frac{S^*}{2} \\ c\xi P_T^* + \hat{\lambda}\frac{S^*}{2} & \hat{\lambda}\frac{S^*}{2} \end{pmatrix} \tag{S4.3}$$

and

$$V = \begin{pmatrix} \mu + bP^* + \hat{\alpha} & 0 \\ 0 & \mu + bP^* + \hat{\alpha} \end{pmatrix} \tag{S4.4}$$

According to the NGT, the mutant's invasion fitness proxy is equal to

$$f(\hat{\lambda}, \lambda) = \rho(FV^{-1}) - 1 = \frac{c\xi P_T^* + \hat{\lambda}S^*}{\mu + bP^* + \hat{\alpha}} - 1 \tag{S4.5}$$

where $\rho(FV^{-1})$ is the spectral radius (the maximum absolute value of all eigenvalues) of the matrix FV^{-1} [24].

If the mutant does not die out due to stochastic effects in the early phase of invasion, it spreads and eventually replaces the resident to become a new resident. This process of gradual trait substitutions proceeds in the direction of the selection gradient (the HT rate increases if the selection gradient is positive and declines if it is negative)

$$\left.\frac{\partial f(\hat{\lambda}, \lambda)}{\partial \hat{\lambda}}\right|_{\hat{\lambda}=\lambda} \tag{S4.6}$$

until it vanishes at an evolutionary singularity λ^*:

$$\left.\frac{\partial f(\hat{\lambda}, \lambda)}{\partial \hat{\lambda}}\right|_{\hat{\lambda}=\lambda=\lambda^*} = 0 \tag{S4.7}$$

By definition, the invasion fitness (S4.5) is zero once $\hat{\lambda} = \lambda$. Using this assumption, the zero selection gradient at the singularity λ^* is equivalent to the condition

$$\frac{S^*(\lambda^*) - \alpha'(\lambda^*)}{\mu + bP^*(\lambda^*) + \alpha(\lambda^*)} = 0 \tag{S4.8}$$

where $\alpha'(\lambda^*)$ is the derivative of the trade-off (4) in the main text with respect to the mutant strategy $\hat{\lambda}$ evaluated at the singular point λ^*. The equality (S4.8) is satisfied when

$$S^*(\lambda^*) = \alpha'(\lambda^*) \tag{S4.9}$$

In order to determine whether such a singularity is a stable endpoint of the evolution, the conditions for evolutionary and convergent stability must be fulfilled [25]. Evolutionary stability ensures resistance of the resident strategy against invasions of neighbouring mutants, and due to convergent stability the evolutionary singularity is reachable by small subsequent mutational steps. A straightforward calculation shows that the evolutionary singularity λ^* is always evolutionary stable

$$\frac{\partial^2 f(\hat{\lambda}, \lambda)}{\partial \hat{\lambda}^2}\bigg|_{\hat{\lambda}=\lambda=\lambda^*} = -\frac{\alpha''(\lambda^*)}{\mu + bP^*(\lambda^*) + \alpha(\lambda^*)} < 0 \tag{S4.10}$$

since the second derivative $\alpha''(\lambda^*)$ of the trade-off (4) in the main text with respect to the mutant trait $\hat{\lambda}$ is always positive. Convergent stability is determined by the condition

$$\frac{\partial^2 f(\hat{\lambda}, \lambda)}{\partial \hat{\lambda}^2} + \frac{\partial^2 f(\hat{\lambda}, \lambda)}{\partial \hat{\lambda} \partial \lambda}\bigg|_{\hat{\lambda}=\lambda=\lambda^*} = \frac{-\alpha''(\lambda^*) + S^{*\prime}(\lambda^*)}{\mu + bP^*(\lambda^*) + \alpha(\lambda^*)} < 0 \tag{S4.11}$$

where $S^{*\prime}(\lambda^*)$ is the derivative of the equilibrium S^* with respect to the resident trait λ evaluated at the singularity λ^*. Once $\alpha''(\lambda^*) > S^{*\prime}(\lambda^*)$, the singularity is also convergent stable.

Appendix S5 Evolution of male-killing efficacy q

Alternatively, we now assume the male-killing efficacy q to be the evolution-undergoing life history trait. Then, the resident-mutant dynamics are as follows:

$$\begin{aligned}
\frac{dS}{dt} &= \frac{2c}{(\frac{S}{2}+F_i+\hat{F}_i)/h+\frac{S}{2}+M_i+\hat{M}_i}\left[\left(\frac{S}{2}+M_i+\hat{M}_i\right)\left(\frac{S}{2}+(1-\xi)(r(q)F_i+r(\hat{q})\hat{F}_i)\right)\right] \\
&\quad -\lambda(F_i+M_i+\hat{F}_i+\hat{M}_i)S-(\mu+bP)S \\
\frac{dF_i}{dt} &= cr(q)\xi\frac{F_i\left(\frac{S}{2}+M_i+\hat{M}_i\right)}{(\frac{S}{2}+F_i+\hat{F}_i)/h+\frac{S}{2}+M_i+\hat{M}_i}+\lambda(F_i+M_i)\frac{S}{2}-(\mu+bP)F_i-\alpha F_i \\
\frac{dM_i}{dt} &= cr(q)\xi(1-q)\frac{F_i\left(\frac{S}{2}+M_i+\hat{M}_i\right)}{(\frac{S}{2}+F_i+\hat{F}_i)/h+\frac{S}{2}+M_i+\hat{M}_i}+\lambda(F_i+M_i)\frac{S}{2}-(\mu+bP)M_i-\alpha M_i \\
\frac{d\hat{F}_i}{dt} &= cr(\hat{q})\xi\frac{\hat{F}_i\left(\frac{S}{2}+M_i+\hat{M}_i\right)}{(\frac{S}{2}+F_i+\hat{F}_i)/h+\frac{S}{2}+M_i+\hat{M}_i}+\lambda(\hat{F}_i+\hat{M}_i)\frac{S}{2}-(\mu+bP)\hat{F}_i-\alpha\hat{F}_i \\
\frac{d\hat{M}_i}{dt} &= cr(\hat{q})\xi(1-\hat{q})\frac{\hat{F}_i\left(\frac{S}{2}+M_i+\hat{M}_i\right)}{(\frac{S}{2}+F_i+\hat{F}_i)/h+\frac{S}{2}+M_i+\hat{M}_i}+\lambda(\hat{F}_i+\hat{M}_i)\frac{S}{2}-(\mu+bP)\hat{M}_i-\alpha\hat{M}_i
\end{aligned} \tag{S5.1}$$

Again, $\hat{F}_i$ and $\hat{M}_i$ denote densities of female and male hosts affected by mutant male-killers, respectively. Calculation of the invasion fitness proxy $f(\hat{q},q)$ of a rare mutant $\hat{q}$ which invades the resident population q at its ecological equilibrium $(S,F_i,M_i,\hat{F}_i,\hat{M}_i)=(S^*,F_i^*,M_i^*,0,0)$ is again based on the sub-matrix J_{mut} of the Jacobian matrix of the model (S5.1), given as

$$J_{mut}=\begin{pmatrix} c\hat{r}\xi P_T^*+\lambda\frac{S^*}{2}-(\mu+bP^*)-\alpha & \lambda\frac{S^*}{2} \\ c\hat{r}(1-\hat{q})\xi P_T^*+\lambda\frac{S^*}{2} & \lambda\frac{S^*}{2}-(\mu+bP^*)-\alpha \end{pmatrix} \tag{S5.2}$$

with the same notation as in Appendix S4.

Again, we decompose the matrix (S5.2) such that $J_{mut}=F-V$ where F is the matrix of all terms representing creation of new infected individuals (birth rates and transitions from the uninfected class to the infected class) and V is the matrix of all terms representing removal of individuals (death rates) [24]. Therefore, we have

$$F=\begin{pmatrix} c\hat{r}\xi P_T^*+\lambda\frac{S^*}{2} & \lambda\frac{S^*}{2} \\ c\hat{r}\xi(1-\hat{q})P_T^*+\lambda\frac{S^*}{2} & \lambda\frac{S^*}{2} \end{pmatrix} \tag{S5.3}$$

and

$$V = \begin{pmatrix} \mu + bP^* + \alpha & 0 \\ 0 & \mu + bP^* + \alpha \end{pmatrix} \tag{S5.4}$$

Obviously, the matrix FV^{-1} is as follows:

$$FV^{-1} = \begin{pmatrix} \frac{c\hat{r}\xi P_T^* + \lambda\frac{S^*}{2}}{\mu + bP^* + \alpha} & \frac{\lambda\frac{S^*}{2}}{\mu + bP^* + \alpha} \\ \frac{c\hat{r}\xi(1-\hat{q})P_T^* + \lambda\frac{S^*}{2}}{\mu + bP^* + \alpha} & \frac{\lambda\frac{S^*}{2}}{\mu + bP^* + \alpha} \end{pmatrix} \tag{S5.5}$$

At the resident's endemic equilibrium, the equation for F_i of the model (S1.2) implies

$$cr\xi F_i^* P_T^* + \lambda\frac{S^*}{2}(F_i^* + M_i^*) - (\mu + bP^* + \alpha)F_i^* = 0 \tag{S5.6}$$

which leads to

$$\frac{1}{\mu + bP^* + \alpha} = \frac{1}{cr\xi P_T^* + \lambda\frac{S^*}{2}}\left(1 - \frac{\lambda\frac{S^*}{2}}{\mu + bP^* + \alpha} \cdot \frac{M_i^*}{F_i^*}\right) \tag{S5.7}$$

Similarly, the equation for M_i of the model (S1.2) implies

$$\frac{1}{\mu + bP^* + \alpha} = \frac{1}{cr\xi(1-q)P_T^* + \lambda\frac{S^*}{2}}\left(\frac{M_i^*}{F_i^*} - \frac{\lambda\frac{S^*}{2}}{\mu + bP^* + \alpha} \cdot \frac{M_i^*}{F_i^*}\right) \tag{S5.8}$$

Plugging the term (S5.7) into the upper left element of the matrix FV^{-1} (S5.5), and the term (S5.8) into the lower left element of the matrix FV^{-1} (S5.5), we get

$$FV^{-1} = \begin{pmatrix} \frac{c\hat{r}\xi P_T^* + \lambda\frac{S^*}{2}}{cr\xi P_T^* + \lambda\frac{S^*}{2}}\left(1 - \frac{\lambda\frac{S^*}{2}}{\mu + bP^* + \alpha} \cdot \frac{M_i^*}{F_i^*}\right) & \frac{\lambda\frac{S^*}{2}}{\mu + bP^* + \alpha} \\ \frac{c\hat{r}\xi(1-\hat{q})P_T^* + \lambda\frac{S^*}{2}}{cr\xi(1-q)P_T^* + \lambda\frac{S^*}{2}}\left(\frac{M_i^*}{F_i^*} - \frac{\lambda\frac{S^*}{2}}{\mu + bP^* + \alpha} \cdot \frac{M_i^*}{F_i^*}\right) & \frac{\lambda\frac{S^*}{2}}{\mu + bP^* + \alpha} \end{pmatrix} \tag{S5.9}$$

The advantage of such a reformulation is that for $\hat{q} = q$ the matrix FV^{-1} reduces to

$$FV^{-1}|_{\hat{q}=q} = \begin{pmatrix} 1 - \frac{\lambda\frac{S^*}{2}}{\mu + bP^* + \alpha} \cdot \frac{M_i^*}{F_i^*} & \frac{\lambda\frac{S^*}{2}}{\mu + bP^* + \alpha} \\ \frac{M_i^*}{F_i^*} - \frac{\lambda\frac{S^*}{2}}{\mu + bP^* + \alpha} \cdot \frac{M_i^*}{F_i^*} & \frac{\lambda\frac{S^*}{2}}{\mu + bP^* + \alpha} \end{pmatrix} \tag{S5.10}$$

It can be relatively easily derived analytically that the spectral radius of (S5.10) is equal to 1, so that $f(q, q) = 0$, as expected.

We use the NGT to estimate the invasion fitness proxy of an invading mutant strain by calculating the dominant eigenvalue $f(\hat{q}, q)$ of the next generation matrix (S5.9), evaluated at the resident endemic equilibrium [24]. And we again apply the techniques of adaptive dynamics theory [25] to determine positivity of the invasion fitness $f(\hat{q}, q)$ of a rare mutant strain $\hat{q}$ in the resident environment q. We focus on finding an evolutionary singularity q^*

corresponding to the zero fitness gradient

$$\left.\frac{\partial f(\hat{q},q)}{\partial \hat{q}}\right|_{\hat{q}=q=q^*}=0 \tag{S5.11}$$

Our model yields three evolutionary endpoints – attracting lower bound $q=0$, attracting upper bound $q=1$, and a branching point which is evolutionary unstable,

$$\left.\frac{\partial^2 f(\hat{q},q)}{\partial \hat{q}^2}\right|_{\hat{q}=q=q^*}>0 \tag{S5.12}$$

and convergent stable singularity,

$$\left.\frac{\partial^2 f(\hat{q},q)}{\partial \hat{q}^2}+\frac{\partial^2 f(\hat{q},q)}{\partial \hat{q}\partial q}\right|_{\hat{q}=q=q^*}<0 \tag{S5.13}$$

Upon arrival at a branching point the evolving bacterium will become dimorphic. Two phenotypically distinct strains will at least initially evolve away from the singularity and apart from one another.

Appendix S6 Additional evolutionary results

Appendix S6.1 Evolution under density-dependent birth

We also tested robustness of the observed evolutionary results with respect to the type of density dependence. Assuming density dependence acts on births rather than deaths, we observe a substantial decrease in λ^*, because opportunities for HT decrease with reduced number of newly born susceptible individuals available to be infected by the parasite (Fig. S 4A). However, the evolution of MK efficacy q stays virtually unaffected (Fig. S 4B-D).

Appendix S6.2 Evolution under concave trade-off $\alpha(\lambda)$ (S2.5)

For the sake of completeness, we investigated evolutionary behaviour of the model (S1.1) also for a concave trade-off $\alpha(\lambda)$ (equation (S2.5) with $a_2>1$). For low to intermediate ξ, λ^* reaches its maximum possible value (Fig. S 5A) and MK does not evolve. For high enough ξ, evolutionary branching in λ occurs, resulting in a stable coexistence of two parasites transmitted horizontally at the maximum HT rate $\lambda_{\max}$ and at the minimum rate $\lambda_{\min}$ (Fig. S 5B). MK then evolves only in a branch transmitted perfectly vertically ($\lambda=\lambda_{\min}$).

Sequential trait evolution is an accurate approximation of the simultaneous trait evolutionary dynamics also for the case of a concave trade-off $\alpha(\lambda)$ (equation (S2.5) with $a_2>1$). For low ξ, MK does not evolve (Fig. S 5C). For high enough ξ, MK can evolve via evolution-

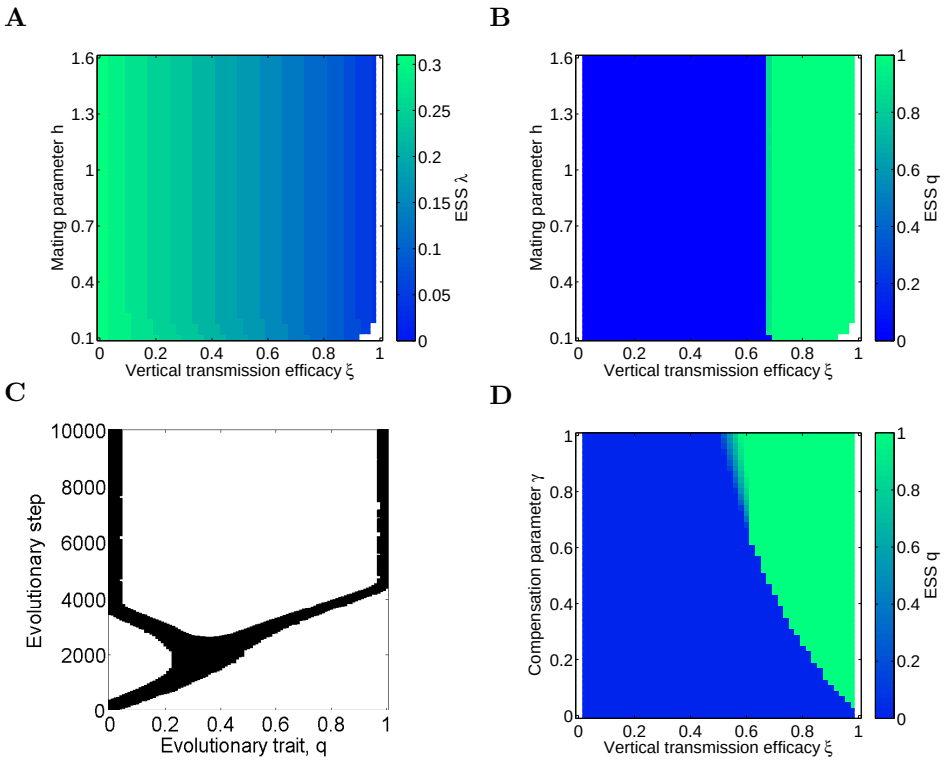

Figure S 4: Sequential trait evolution when the VT efficacy ξ is fixed and density dependence acts on the host birth rate. The types of evolutionary endpoints and the colour legend are identical as in Fig. 1 in the main text. (C) An example of evolutionary branching. Parameters: (B) $\gamma = 0.5$, (C) $\xi = 0.6$, $\gamma = 0.72$, $\lambda^* = 0.15$, (C-D) $h = 1$. Common parameters: $b = 0$, $k = 1$, $a_2 = 0.5$. All other parameters are given in Table S 1.

ary branching (Fig. S 5D) following evolutionary branching in the HT rate λ. Two strains ($\lambda = \lambda_{\min}, q = 1$) and ($\lambda = \lambda_{\max}, q = 0$) stably coexist.

Appendix S6.3 Sequential trait evolution when VT efficacy ξ and HT rate λ are linked via trade-off (S2.6)

We now assume that the parasite is allowed to control the efficacy of its VT, i.e. that ξ and λ are linked via the trade-off (S2.6) (Fig. S 6A). If VT is quite costly ($0 < z << 1$), we observe evolution towards an attractor λ^* (and thus low VT) (Fig. S 6B). If VT is only moderately costly ($0 << z < 1$), evolutionary branching in λ occurs with one strain being transmitted at the minimum HT rate $\lambda_{\min}$ (and thus the maximum VT efficacy $\xi_{\max}$) and the other with a low HT rate (and thus a high VT efficacy) (Fig. S 6C). Finally, if VT is cheap ($z > 1$), the parasite settles near its minimum HT rate (and thus almost perfect VT) (Fig. S 6D). Here, we again observe evolution towards high rates of HT in polygynous mating systems (results not shown). The MK ability does not evolve for convex trade-offs (S2.6) and costly VT (i.e. $0 < z << 1$, Fig. S 6E). On the contrary, an almost fully efficient male-killer evolves if the trade-off (S2.6) is either slightly convex and VT is moderately costly (i.e. $0 << z < 1$,

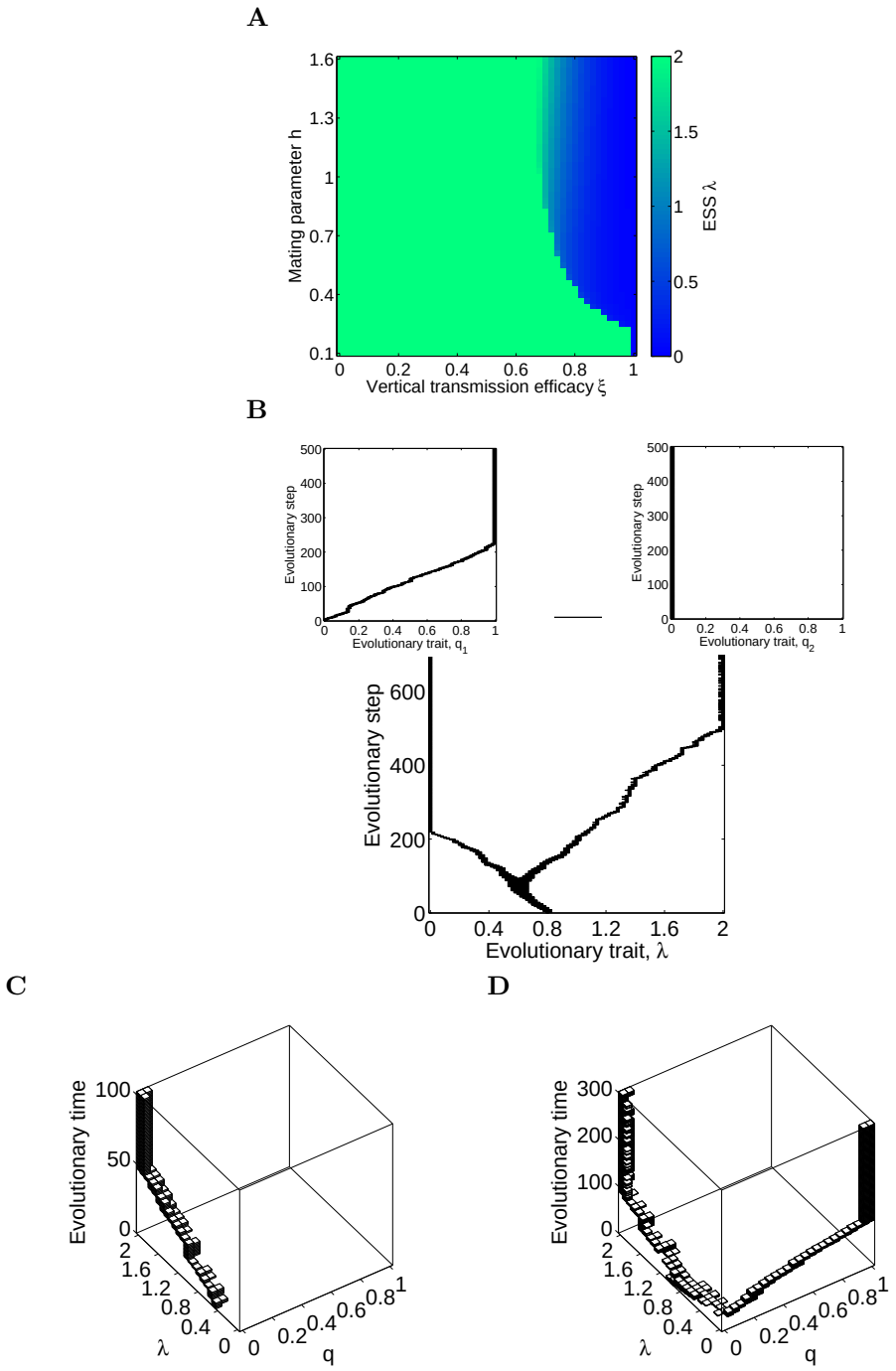

Figure S 5: Trait evolution for the concave trade-off $\alpha(\lambda)$ (equation (4) in the main text). (A) An attracting upper bound $\lambda_{\max}$ (pure green) or a branching point as an evolutionary outcome for λ^*. (B) An example of evolutionary branching in λ and subsequent evolution of male-killing efficacy q in both branches. (C)-(D) An example of a simultaneous evolution of λ and q. Parameters: (B) $\xi = 0.8$, (C) $\xi = 0.3$, (D) $\xi = 0.8$, (C-D) $\lambda_{\min} = 0$, $\lambda_{\max} = 2$. Common parameters: $\gamma = 0.5$, $h = 1$, $a_2 = 2$. All other parameters are given in Table S 1.

Fig. S 6F) or the trade-off (S2.6) is concave and VT is cheap ($z > 1$, Fig. S 6G).

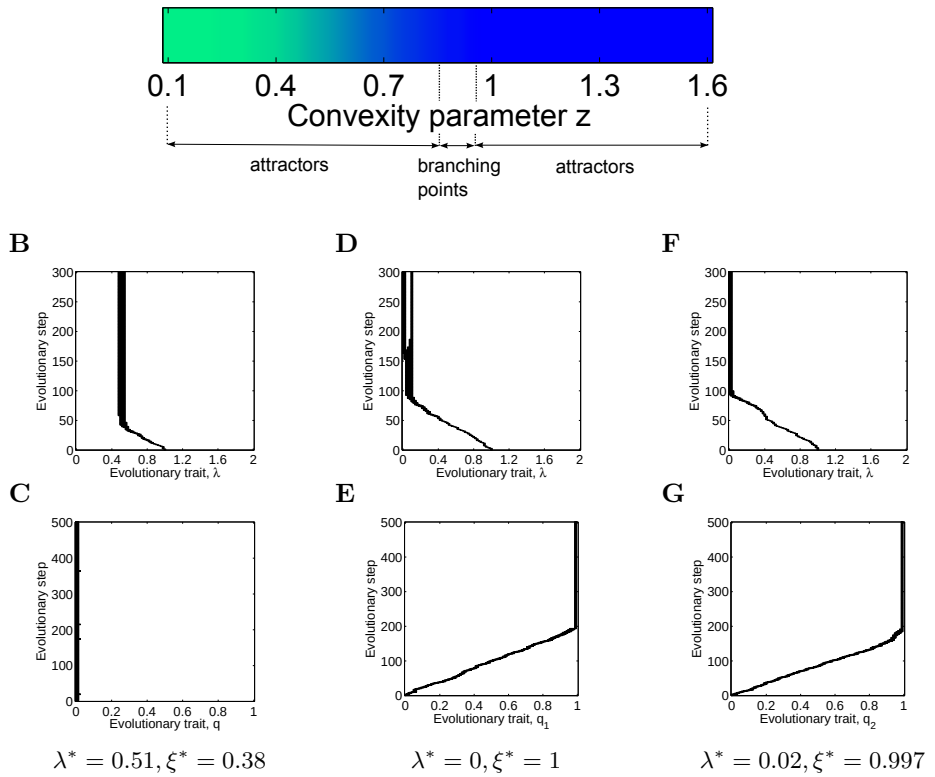

Figure S 6: Sequential trait evolution when VT efficacy ξ and HT rate λ are linked via trade-off (S2.6). (A) Evolutionary endpoints λ for $h = 1$ as they vary along the trade-off ((S2.6)) with convexity parameter z. (B) Evolutionary attractor λ^*, for $z = 0.6$. (C) Subsequent evolution of MK at λ^*, for $z = 0.6$; the parasite does not evolve any MK ability and settles at $q^* = 0$. (D) Evolutionary branching in a singularity λ^*, for $z = 0.9$. (E) Subsequent evolution of MK in a surviving branch $\lambda^* = 0$, for $z = 0.9$; the second branch with $\lambda^* > 0$ dies out once the parasite stars evolving the MK. The parasite evolves almost full MK ability with $q^* = 0.99$. (F) Evolutionary attracting lower bound $\lambda_{\min} = 0$ maintains itself due to the presence of a parasite with a slightly higher HT rate $\lambda^* = 0.02$; $z = 1.2$. (G) Subsequent evolution of MK for $\lambda^* = 0.02$, for $z = 1.2$; the parasite with $\lambda = \lambda_{\min}$ dies out once MK starts evolving in both strains. The parasite evolves almost full MK ability with $q^* = 0.99$. Common parameters: $\lambda_{\min} = 0$, $\lambda_{\max} = 2$, $\xi_{\min} = 0$, $\xi_{\max} = 1$, $\gamma = 0.5$, $h = 1$, $a_2 = 0.5$. All other parameters are given in Table S 1.

Appendix S7 Simulation model for simultaneous trait evolution

Here we describe how we numerically simulated simultaneous evolution of two bacterial traits, the horizontal transmission rate λ and the male-killing efficacy q. We discretized the range $[0, 1]$ for q into 25 values (initial value 0, step 0.04, final value 1) and the range $[\lambda_{\min}, \lambda_{\max}]$ for λ also into 25 values (initial value $\lambda_{\min}$, step $(\lambda_{\max} - \lambda_{\min})/25$, final value $\lambda_{\max}$), thus considering $(25)^2 = 625$ possible bacterium phenotypes that may occur during

evolution. The core model of the simulations is thus a system of $2(25)^2 + 1 = 1251$ ordinary differential equations; one equation for susceptible individuals, and one equation for infected females and one equation for infected males for each phenotype. This system of equations is actually a combination of models (S4.1) and (S5.1).

The evolutionary simulation proceeds as follows. We start with a single phenotype; a positive initial density is assigned to this phenotype, while initial densities of all the other phenotypes are set to zero. We then run the core model for a fixed amount of time, here set to 300. This particular time span, found by running many diverse simulations, appears sufficiently long for the ecological dynamics of the population to settle at a stable equilibrium. In line with the assumptions of adaptive dynamics theory, we split the ecological and evolutionary time-scales and let the ecological dynamics stabilize before any new mutant appears in the population. The ecological time span, together with mutations at its end (see below), form one evolutionary step. After the ecological dynamics stabilize and before any new mutations occur, bacterial strains whose density falls below a critical value (here set to 10^{-10}) are presumed extinct and their density is set to zero.

Next, we choose a persistent strain, based on relative densities of all persistent strains, to generate a mutant. The mutant has a trait neighbouring to the strain chosen; with equal probability we take the neighbouring left value or the neighbouring right value from our ordered list of 25 discrete values. If the mutant value does not exist (e.g. if we are expected to take the closest left value for q of the strain with zero male-killing efficacy), no mutation in the respective trait occurs at that moment. Any mutant strain is initiated at a low density, which is subtracted from the density of its parent strain. Mutations in q and λ occur independently, so that one strain is selected for mutation in q and one (which may by chance be the same as the first one) for mutation in λ. Simulation is run for a given number of evolutionary steps, until an evolutionary endpoint is attained.

Since we choose just two strains to mutate at the end of each evolutionary step, mutations are independent of the number or density of infected hosts. Again, this is assumed to fit the assumptions of adaptive dynamics theory, by splitting the ecological and evolutionary time-scales. On the other hand, we also conducted simulations with both shorter and longer evolutionary steps than 300 time units. This corresponded to faster and slower mutation rates, respectively. However, the resulting evolutionary trees stayed always qualitatively the same. Our results thus do not seem to depend on whether mutations are dependent on or independent of the number or density of infected hosts.

Numerical simulations were run in Matlab (The MathWorks, Inc., release R2009b). To solve the system of $2(25)^2+1 = 1251$ ordinary differential equations in a reasonable time, we

used the sundialsTB package (computation.llnl.gov/casc/sundials) with the Adams method. The full simulation code is available upon request from the authors.

References

[1] L. D. Hurst. The incidences and evolution of cytoplasmic male killers. *Proc R Soc B*, 244:91–99, 1991. doi: 10.1098/rspb.1991.0056.

[2] G. D. D. Hurst, E. L. Purvis, J. J. Sloggett, and M. E. N. Majerus. The effect of infection with male-killing *Rickettsia* on the demography of female *Adalia bipunctata* L. (two spot ladybird). *Heredity*, 73:309–316, 1994. doi: 10.1038/hdy.1994.138.

[3] G. D. D. Hurst and F. M. Jiggins. Male-killing bacteria in insects: mechanisms, incidence, and implications. *Emerg Infect Dis*, 6:329–336, 2000. doi: 10.3201/eid0604.000402.

[4] M. A. C. Groenenboom and P. Hogeweg. Space and the persistence of male-killing endosymbionts in insect populations. *Proc R Soc B*, 269:2509–2518, 2002. doi: 10.1098/rspb.2002.2197.

[5] M. van Baalen and M. W. Sabelis. The dynamics of multiple infection and the evolution of virulence. *Am Naturalist*, 146:881–910, 1995. doi: 10.1086/285830.

[6] M. Choisy and J. C. de Roode. Mixed infections and the evolution of virulence: effects of resource competition, parasite plasticity, and impaired host immunity. *Am Naturalist*, 175:E105–118, 2010. doi: 10.1086/651587.

[7] B. R. Levin and R. E. Lenski. Coevolution in bacteria and their viruses and plasmids. In D. J. Futuyma and M. Slatkin, editors, *Coevolution*, pages 99–127. Sinauer Associates Inc, Sunderland, Massachusetts, 1983.

[8] R. M. May and R. M. Anderson. Epidemiology and genetics in the coevolution of parasites and hosts. *Proc R Soc B*, 219:281–313, 1983. doi: 10.1098/rspb.1983.0075.

[9] F. van den Bosch, B. A. Fraaije, F. van den Berg, and M. W. Shaw. Evolutionary bi-stability in pathogen transmission mode. *Proc R Soc B*, 277:1735–1742, 2010. doi: 10.1098/rspb.2009.2211.

[10] J. E. Ironside, J. E. Smith, M. J. Hatcher, and A. M. Dunn. Should sex-ratio distorting parasites abandon horizontal transmission? *BMC Evol Biol*, 11:370, 2011. doi: 10.1186/1471-2148-11-370.

[11] V. Bernhauerova and L. Berec. Role of trade-off between sexual and vertical routes for evolution of pathogen transmission. *Theor Ecol*, 8:23–36, 2015. doi: 10.1007/s12080-014-0234-8.

[12] P. X. Kover and K. Clay. Trade-off between virulence and vertical transmission and the maintenance of a virulent plant pathogen. *Am Naturalist*, 152:165–175, 1998. doi: 10.1086/286159.

[13] A. D. Stewart, J. M. Logsdon jr., and S. E. Kelley. An empirical study of the evolution of virulence under both horizontal and vertical transmission. *Evolution*, 59:730–739, 2005. doi: 10.1554/03-330.

[14] P. E. Turner, V. S. Cooper, and R. E. Lenski. Tradeoff between horizontal and vertical modes of transmission in bacterial plasmids. *Evolution*, 52:315–329, 1998. doi: 10.2307/2411070.

[15] P. E. Turner. Phenotypic plasticity in bacterial plasmids. *Genetics*, 167:9–20, 2004. doi: 10.1534/genetics.167.1.9.

[16] S. T. Emlen and L. W. Oring. Ecology, sexual selection, and the evolution of mating systems. *Science*, 197:215–223, 1977. doi: 10.1126/science.327542.

[17] F. M. Jiggins, G. D. D. Hurst, and M. E. N. Majerus. Sex-ratio-distorting *Wolbachia* causes sex-role reversal in its butterfly host. *Proc R Soc B*, 267:69–73, 2000. doi: 10.1098/rspb.2000.0968.

[18] S. Charlat, G. D. D. Hurst, and H. Mercot. Evolutionary consequences of *Wolbachia* infections. *Trends Genet*, 19:217–223, 2003. doi: 10.1016/S0168-9525(03)00024-6.

[19] S. Charlat, G. D. D. Hurst, and H. Mercot. Male-killing bacteria trigger a cycle of increasing male fatigue and female promiscuity. *Curr Biol*, 17:273–277, 2007. doi: 10.1016/j.cub.2006.11.068.

[20] H. Caswell and D. E. Weeks. Two-sex models: chaos, extinction, and other dynamic consequences of sex. *Am Naturalist*, 128:707–735, 1986. doi: 10.1086/284598.

[21] M. R. Miller, A. White, K. Wilson, and M. Boots. The population dynamical implications of male-biased parasitism in different mating systems. *PLoS One*, (7):e624, 2007. doi: 10.1371/journal.pone.0000624.

[22] T. E. X. Miller and B. D. Inouye. Confronting two-sex demographic models with data. *Ecology*, 92:2141–2151, 2011. doi: 10.1890/11-0028.1.

[23] L. Berec and D. Maxin. Why have parasites promoting mating success been observed so rarely? *J Theor Biol*, 342:47–61, 2014. doi: 10.1016/j.jtbi.2013.10.012.

[24] A. Hurford, D. Cownden, and T. Day. Next-generation tools for evolutionary invasion analyses. *J R Soc Interface*, 7:561–571, 2010. doi: 10.1098/rsif.2009.0448.

[25] S. A. H. Geritz, E. Kisdi, G. Meszena, and J. A. J. Metz. Evolutionarily singular strategies and the adaptive growth and branching of the evolutionary tree. *Evol Ecol*, 12:35–57, 1998. doi: 10.1023/A:1006554906681.

List of tables

Parameter	Meaning	Value
q	Probability of male-killing during embryogenesis	varies
r	Fitness enhancement factor due to male-killing	varies
λ	Horizontal transmission rate of the bacterium	varies
$\lambda_{\min}$	Minimal horizontal transmission rate of the bacterium	varies
$\lambda_{\max}$	Maximal horizontal transmission rate of the bacterium	varies
α	Disease-induced mortality rate (virulence)	varies
c	Per-mating number of offspring (birth rate)	3
μ	Intrinsic per capita mortality rate	0.1
b	Strength of density dependence in the mortality rate	0.1
ξ	Vertical transmission efficacy of the bacterium	varies
$\xi_{\min}$	Minimal vertical transmission efficacy of the bacterium	varies
$\xi_{\max}$	Maximal vertical transmission efficacy of the bacterium	varies
h	Constant that determines the type of mating system	varies
γ	Constant that determines shape of the trade-off (S2.1)	varies
a_1	Constant that determines shape of the trade-off (S2.3)	1
a_2	Constant that determines shape of the trade-off (S2.3)	0.5 or 2
k	Strength of density dependence in the birth rate	0 or 1

Table S 1: Parameters used in the model (1).

pairs / offspring	F_i	F_u	M_i	M_u
F_iM_u	$r^* \frac{\xi}{2}$	$r \frac{1-\xi}{2}$	$(1-q)r \frac{\xi}{2}$	$r \frac{1-\xi}{2}$
F_iM_i	$r \frac{\xi}{2}$	$r \frac{1-\xi}{2}$	$(1-q)r \frac{\xi}{2}$	$r \frac{1-\xi}{2}$
F_uM_u	–	$1/2$	–	$1/2$
F_uM_i	–	$1/2$	–	$1/2$

* An infected offspring that comes from an infected female benefits from enhanced survival represented by the factor r. See Table 1 in the main text for meaning of the other parameters.

Table S 2: Probability that a pair produces either infected or uninfected female/male offspring.